

A Polytopic Box Particle Filter for state estimation of Non Linear Discrete-Time Systems

Thomas Gatto* Luc Meyer* H el ene Piet-Lahanier*

* *D epartement Traitement de l'Information et Syst emes, ONERA,
Univ Paris Saclay, Palaiseau*

Abstract: The development of Particle Filters has made possible state estimation of dynamic systems presenting non-linear dynamics and potential multi-modalities. However, the efficiency of these approaches depends tightly of the required number of particles which may prove very high to approximate large range of uncertainty on the process or the measurements. To overcome this issue, the Box-Particle Filter (BPF) combines the versatility of the Particle Filter and the robustness of set-membership algorithms. The particles are replaced by boxes which represent in a compact way large variations of the estimates. Although this filter presents various advantages and requires a small number of boxes to estimate the state, the resulting estimates may prove pessimistic, as the uncertainty description as unions of axis-aligned intervals can be rather rough and doesn't account for potential dependencies between the resulting estimate components. In the proposed paper, a new version of the BPF is proposed. Boxes are replaced by polytopes (multidimensional polygons) in the filter algorithm, so that they can adapt to represent state components dependency. This modification tends to ameliorate the estimation precision (i.e. the size of the final set that includes the true state decreases) while keeping the number of required polyhedrons small. Several examples illustrate the benefits of such an approach.

Keywords: Particle Filter, Intervals, Polytopes, Estimation, Bounded noise, Set-Membership uncertainty, Uncertain dynamic systems.

1. INTRODUCTION

State estimation of dynamic systems is commonly addressed by modelling the uncertainty as a stochastic variable, usually assumed Gaussian. For linear or non-linear systems, such problems are solved by using a classical (KF) (Kalman et al. (1960)), an extended (EKF) or an unscented (UKF) Kalman Filter (Julier and Uhlmann (1997)). For non-linear systems, particle filters have been developed to tackle non-Gaussian non-unimodal noise distributions as described in Van Der Merwe et al. (2001). These filters prove efficient for various applications but suffer from the drawback that the number of particles required to describe large variations of uncertainty on the dynamics or the measurements can become very high. Moreover, stochastic representation of errors is not immune to criticism as the probability density function is seldom known a priori. In set-membership estimation, process and measurement uncertainties are only assumed to vary within known bounds which makes this type of approach very robust to lack of probabilistic information. Various set structures have been used to characterize the variation domain of the system states, given the model structure and bounds as for example proposed in Jaulin (2001); Bo et al. (2013); Polyak et al. (2004); Scholte and Campbell (2003). However, this characterization results often in a pessimistic estimation, especially for multi-modal distributions. A more recent alternative method, first introduced by Abdallah et al. (2008) consists in com-

bining the versatility of the particle representation with the robustness of set-membership method. This translates in replacing the point particle by a box which results in reducing significantly the number of particles and the adverse effects of non-linearity. Box Particle Filter (BPF) estimators have already been applied in Simultaneous Localization and Mapping (SLAM) as in Abdallah et al. (2008), or mobile localization as in Wang et al. (2018). However, the BPF provides a rather pessimistic solution due to the fact that the boxes have to be aligned along the state axes which result in losing potential dependencies between the resulting estimate components. Moreover, its significant computational cost is another inconvenient which is mainly due to the contraction part of the algorithm.

To address those issues, an improvement of the box description could be to combine this description with a more precise and versatile set characterization using polyhedral boundaries as in Walter and Piet-Lahanier (1989). The aim of this paper is to consider polyhedral set description instead of boxes in the measurement update step of the filter. The idea is that the description of a set using polyhedral rather than boxes can be tightened to fit closely to the set of measurement leading to a more precise description, and thus a better state estimation.

The paper is organized as follows. The problem addressed is described in section 2. The modified box particle filter algorithm is then presented in section 3. Examples of

application are presented in section 4, with comparisons with the Box Particle Filter. Conclusion on the results and future work terminates the paper.

2. PROBLEM STATEMENT

Let consider the following non linear discrete-time system:

$$\begin{cases} x_{k+1} = f(x_k) + w_k \\ y_k = h(x_k) + v_k \end{cases}, \quad (1)$$

where $x_k \in \mathbb{R}^{n_x}$ is the state vector and $y_k \in \mathbb{R}^{n_y}$ the measurement vector, n_x and n_y denoting their respective dimensions. The function $f: \mathbb{R}^{n_x} \rightarrow \mathbb{R}^{n_x}$ is a non-linear *state transition function* defining the state at time $k + 1$ from the previous state at time $k \in \mathbb{N}$ and $w_k \in \mathbb{R}^{n_x}$ a process noise vector. The function $h: \mathbb{R}^{n_x} \rightarrow \mathbb{R}^{n_y}$ is a non-linear *measurement function* defining the relation between the state and the measurement at time k and $v_k \in \mathbb{R}^{n_y}$ is an additive measurement noise vector.

Knowing the functions f and h , the aim of the filter proposed in this paper is to estimate recursively the state vectors x_k at each time step $k > 0$, using a first guess of x_0 , as well as, the successive measurement vectors y_k .

When the disturbance terms w_k and v_k follow a known stochastic distribution, a solution to such a problem is to use the well-known particle filter.

In our case, the disturbances are no more assumed to follow such a distribution. The only assumption made is that they are bounded. More precisely we consider the following assumption.

Assumption 1. The disturbance terms w_k and v_k are assumed to be unknown but bounded (UBB) noises, i.e. for each $k \geq 0$, it exists n_w positive scalars $\varepsilon_{k,i}^w, i \in \{1, \dots, n_w\}$, and n_v positive scalars $\varepsilon_{k,i}^v, i \in \{1, \dots, n_v\}$, such that:

$$\|w_{k,i}\| \leq \varepsilon_{k,i}^w, i = 1, \dots, n_w \iff \|w_k\|_\infty^{\varepsilon_k^w} \leq 1, \quad (2)$$

$$\|v_{k,i}\| \leq \varepsilon_{k,i}^v, i = 1, \dots, n_v \iff \|v_k\|_\infty^{\varepsilon_k^v} \leq 1, \quad (3)$$

where, for any vector $\varepsilon \in \mathbb{R}^n$ with positive components and any vector $u \in \mathbb{R}^n$, the norm $\|\cdot\|_\infty$ is defined as:

$$\|u\|_\infty^\varepsilon = \max_{i=1, \dots, n} \left\{ \frac{u_i}{\varepsilon_i} \right\}. \quad (4)$$

When such an assumption, is made the Box Particle Filter provides a solution to the proposed estimation problem. This filter follow the same steps as the classical particle filter, but is based on the propagation of intervals and boxes (instead of point-wise particles).

Definition 1. A real interval, denoted $[x]$, is defined as a closed and connected subset of \mathbb{R} and an interval (or a box) $[X]$ of \mathbb{R}^{n_x} is defined as a Cartesian product of n_x intervals: $[X] = [x_1] \times [x_2] \times \dots \times [x_{n_x}] = \times_{i=1}^{n_x} [x_i]$. The size of $[X]$ is denoted as $|[x]|$ and is calculated as the product of the respective sizes of all the scalar intervals $[x_i], i = 1, \dots, n_x$.

Associated to intervals, we also define the notion of *inclusion function*.

Definition 2. The inclusion function $[f]$ of a function f is such as the image by $[f]$ of an interval $[x]$ is the minimum size interval $[f]([x])$, containing $f(x)$ for any $x \in [x]$ (more on this in Jaulin (2001)).

Such an approach using boxes has an interest when the measurements are known to belong to some bounded intervals, without any other information.

In the present paper, the BPF is improved by replacing temporarily the boxes by polytopes. It has an interest when the different measurement variables are not independent, and thus, the global measurement set is not oriented along the main axis. Indeed, in that case, the BPF approach may be very pessimistic.

Definition 3. An n -dimensional polytope P is defined as a set of n_p vertices $\mathbb{V}_i, i = 1, \dots, n_p$; n_h supporting hyper-planes \mathbb{H}_j ; and n_p lists which contain for each vertex, the indices of its supporting hyper-planes.

Each of the n_h hyper-planes is defined by $\{x \in \mathbb{R}^n | a_i x = b_i\}$, where $a_i^T \in \mathbb{R}^n$ and $b_i \in \mathbb{R}$. Therefore, a n -dimensional polytope P supporting n_h hyper-planes is defined by :

$$\{x \in \mathbb{R}^n | Ax \leq b\}, \quad (5)$$

where $A \in \mathbb{R}^{n_h \times n}$, a_i the i -th row of A , $b \in \mathbb{R}^{n_h}$ and b_i the i -th component of b .

3. PROPOSED ALGORITHM

The objective of the present section is to detail the proposed algorithm, and to emphasize the differences of this former with the classical Box Particle Filter (BPF). Note that the differences between the classical Particle Filter and the Box Particle Filter are detailed in Abdallah et al. (2008).

As said before, the main originality of the proposed algorithm is to use polytopes instead of classical intervals. In a classical BPF, the feasible set is covered by boxes. In our algorithm, this set is covered by polytopes.

The interest of such an approach is that the use of boxes can be quite pessimistic in comparison with the use of polytopes (as it will be seen later).

The global structure of the algorithm and its division in specific steps are similar to the ones of the BPF. The rest of the present section is devoted to the detailed description of this algorithm.

1 Initialization

Let consider the initial box $[X_1]$ to which the initial state is assumed to belong. Note that in some application, when the initial conditions are not known, this box can be chosen arbitrary large.

As in the BPF, the initialization of the filter consists in creating N_p non intersecting boxes $\{[x^i]\}_{i=1}^{N_p}$ with equivalent weights from the initial box $[X_1]$.

2 Prediction

This step is similar for the proposed algorithm and the BPF. The aim is to propagate the box particles $[x_k^i], i = 1, \dots, N_p$ throughout the prediction equation, in order to obtain N_p predicted box particles: $[x_{k+1|k}^i] = [f]([x_k^i]) + [w_k], i = 1, \dots, N_p$.

3 Measurement update

In the classical BPF, the measurement update provides, for each box, the minimum-size box compatible with the

predicted box and the measurement, that is the minimum-size box $[x_{k+1}^i]$ containing the set $\{x \in \mathbb{R}^{n_x} | h(x) - y_k \in [v_k]\}$ (calculation detailed in Abdallah et al. (2008)).

In the proposed algorithm, the observation function h is linearized using first order expansion as in Scholte and Campbell (2003) at the center $x_{k+1|k}^i$ of each predicted box:

$$h(x_k) = h(x_{k+1|k}^i) + C_k(x_k - x_{k+1|k}^i) + o_k, \quad (6)$$

where $C_k = \frac{\partial h(x_{k+1|k}^i)}{\partial x}$ and o_k is the linearization error. Bounds of o_k can be obtained thanks to DC programming (Bo et al. (2013)).

For each measurement y_k and each predicted box $[x_{k+1|k}^i]$, two bounding hyperplanes are defined as:

$$\begin{cases} \underline{\mathcal{H}}_k = \{x \in \mathbb{R}^{n_x} | \\ h(x_{k+1|k}^i) + C_k(x - x_{k+1|k}^i) = y_k - \max([m_k])\} \\ \overline{\mathcal{H}}_k = \{x \in \mathbb{R}^{n_x} | \\ h(x_{k+1|k}^i) + C_k(x - x_{k+1|k}^i) = y_k - \min([m_k])\} \end{cases}, \quad (7)$$

where $[m_k] = [o_k] + [v_k]$.

Using the approach described in Walter and Piet-Lahanier (1989), the measurement update step consists in computing the feasible polytope for each particle by intersecting the predicted box particles with the two half spaces associated with each of the bounding hyperplanes:

$$P_{k+1}^i = [x_{k+1|k}^i] \cap \underline{\mathcal{H}}_k \cap \overline{\mathcal{H}}_k. \quad (8)$$

4 Weights update

In the BPF case, the weight of each particle is updated as:

$$w_{k+1}^i = A_{k+1}^i w_k^i, \quad \forall i \in \{1, \dots, N_p\} \quad (9)$$

where

$$A_{k+1}^i = \frac{|[z_{k+1}^i] \cap [y_{k+1}]|}{|[z_{k+1}^i]|}, \quad (10)$$

with $[z_{k+1}^i] = [h]([x_{k+1|k}^i])$, the predicted box measurement particle, and $[y_{k+1}]$ the (real) box measurement at time step $k+1$.

In the proposed filter, the weight of each particle is updated following (9) but (10) is replaced by:

$$A_{k+1}^i = \frac{V(P_{k+1}^i)}{|[x_{k+1|k}^i]|}, \quad (11)$$

where $V(P_{k+1}^i)$ is the volume of the polytope P_{k+1}^i . This choice is justified in order to favor the particles covering all the measurements.

Note that recursive expressions of the volume of a n -dimensional polytope are given in Lasserre (1983) and Von Hohenbalken (1978), and can be used as weight for each polytopic particle. In the simulations presented in section 4, the Lasserre's method is used (Lasserre (1983)), as it is computationally more effective, and easy to implement (especially in our case where the polytopes are defined by an expression of the form $\{x | Ax \leq b\}$ where each row of A and b characterizes an hyperplane).

At the end of this step, weights are normalized:

$$w_{k+1}^i = \frac{w_{k+1}^i}{\sum_{i=1}^{N_p} w_{k+1}^i}. \quad (12)$$

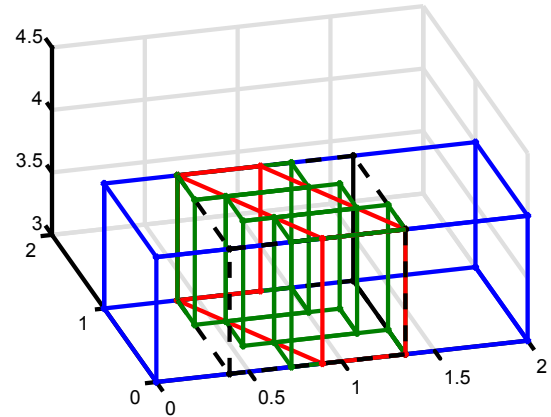


Fig. 1. Measurement update using polytopes (blue: predicted box, red: half spaces associated with each of the bounding hyperplans, green: set of new boxes after resampling, black: set that would be obtained with the BPF)

5 Estimation

At time step k , the new estimated state is computed as

$$\hat{x}_k = \sum_{i=1}^{N_p} w_k^i C_k^i, \quad (13)$$

where in the BPF, C_k^i is the center of the box particle i . In the proposed filter, C_k^i is computed as the barycenter of the polytope i vertices: $C_k^i = \frac{1}{n_p} \sum_{j=1}^{n_p} \mathbb{V}_{k,j}^i$ where $\mathbb{V}_{k,j}^i$ is the j -th vertex of the polytope i at time k . A more accurate way of estimating the new state would be to calculate the barycenter of the polytope, but such a method can be very complex to implement and time-consuming (in Warren (1996)).

Similarly to the BPF, the associated covariance matrix is given by $\hat{P}_k = \sum_{i=1}^{N_p} w_k^i (\hat{x}_k - x_k^i)(\hat{x}_k - x_k^i)^T$.

6 Resampling

The resampling phase consists in eliminating polytopes associated with the lowest weights, and in dividing the polytopes associated with the highest weights. After selection of the polytopes to be kept, each of those is approximated by the smallest box containing it.

Figure 1 illustrates the measurement update and resampling phases. It can be seen that the polyhedral update (in green) makes the resulting estimation uncertainty less pessimistic than with the classical Box Resampling (in black).

4. ILLUSTRATIVE EXAMPLES

In this section, two examples of non linear model estimation are considered in order to evaluate the average precision improvement resulting from the use of the new method.

4.1 Example 1

In order to compare the proposed filter with the BPF, let consider the following 2D non linear system (from Gordon et al. (1993), where a range-measurement has been added):

$$X_{k+1} = \Phi X_k + \Gamma w_k \quad (14)$$

where $X_k = (x, \dot{x}, y, \dot{y})^T$ is the state vector, with (x, y) is the 2D- position, and (\dot{x}, \dot{y}) the associated velocity in a chosen frame, $w_k = (w_x, w_y)_k^T$ is the state noise

(modeling the discretization error), $\Phi = \begin{bmatrix} 1 & \Delta t & 0 & 0 \\ 0 & 1 & 0 & 0 \\ 0 & 0 & 1 & \Delta t \\ 0 & 0 & 0 & 1 \end{bmatrix}$ and

$$\Gamma = \begin{bmatrix} 0.5 & 0 \\ 1 & 0 \\ 0 & 0.5 \\ 0 & 1 \end{bmatrix}, \text{ with } \Delta t \text{ the constant time step.}$$

The measurement vector is defined as $y_k = \begin{bmatrix} \theta_k \\ d_k \end{bmatrix}$, where θ_k and d_k are noisy measurements of the target bearing and range from the origin of the plane:

$$\theta_k = \arctan\left(\frac{y_k}{x_k}\right) + v_k^\theta, \quad (15)$$

$$d_k = \sqrt{x_k^2 + y_k^2} + v_k^d. \quad (16)$$

The system and measurement noises, respectively w_k and $v_k = [v_k^\theta, v_k^d]^T$, are zero mean Gaussian white noises with covariance matrices $E[w_k w_k^T] = Q \delta_{kj}$ and $E[v_k v_k^T] = R \delta_{kj}$, where $Q = q I_2$ (I_2 being the 2×2 identity matrix) and $R = \begin{bmatrix} r^\theta & 0 \\ 0 & r^d \end{bmatrix}$. At time $k = 1$, the initial state vector is assumed to have a Gaussian distribution with known

mean \bar{X}_1 and covariance matrix $M_1 = \begin{bmatrix} \sigma_1^2 & 0 & 0 & 0 \\ 0 & \sigma_2^2 & 0 & 0 \\ 0 & 0 & \sigma_3^2 & 0 \\ 0 & 0 & 0 & \sigma_4^2 \end{bmatrix}$.

Therefore, the boxes initialization is :

$$[X_1] = \begin{bmatrix} x_1 \\ \dot{x}_1 \\ y_1 \\ \dot{y}_1 \end{bmatrix} = \begin{bmatrix} [\bar{x}_1 - 3\sigma_1, \bar{x}_1 + 3\sigma_1] \\ [\bar{\dot{x}}_1 - 3\sigma_2, \bar{\dot{x}}_1 + 3\sigma_2] \\ [\bar{y}_1 - 3\sigma_3, \bar{y}_1 + 3\sigma_3] \\ [\bar{\dot{y}}_1 - 3\sigma_4, \bar{\dot{y}}_1 + 3\sigma_4] \end{bmatrix}.$$

Indeed, in order to convert a Gaussian distribution into a bounded set, we consider that the support of the distribution is limited to the interval $[\bar{x} - 3\sigma; \bar{x} + 3\sigma]$, where \bar{x} is the mean of the distribution, and σ is the standard deviation (in fact 99.73% of the density is concentrated on that interval).

The simulations have been done with the parameter values: $\sqrt{q} = 0.001$, $\sqrt{r^\theta} = 0.005$, $\sqrt{r^d} = 0.05$, $\Delta t = 1$, $\sigma_1 = 0.5$, $\sigma_2 = 0.005$, $\sigma_3 = 0.3$, $\sigma_4 = 0.01$. The initial state is $\bar{X}_1 = (40, 10, 40, -10)^T$.

The subdivision resampling leads to a more precise solution by dividing the boxes and refining the estimation. However, in this example, two state variables are not directly measured so their intervals become wider and wider. To face this problem, boxes are divided until the width of those intervals are less than a fixed quantity. However, if the subdivision occurs just on the non-measured variables, it means that there is no gain in terms of volume reduc-

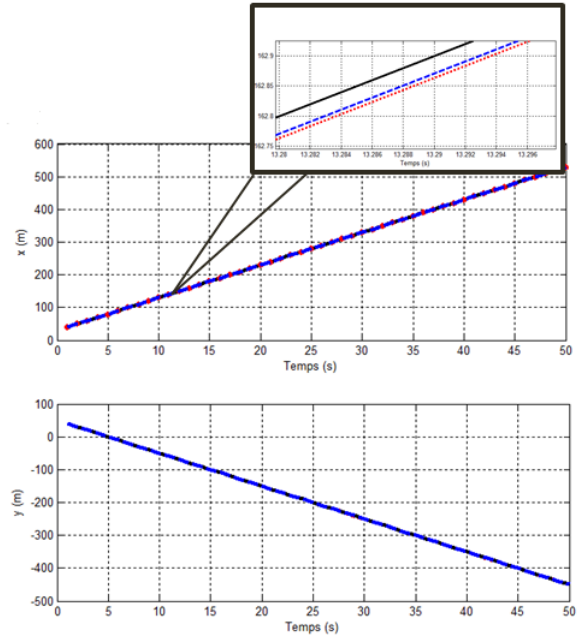


Fig. 2. Example 1: Evolution of the position (x above and y below) with a zoom on the top. Black: Real position. Red: BPF. Blue: PBPf.

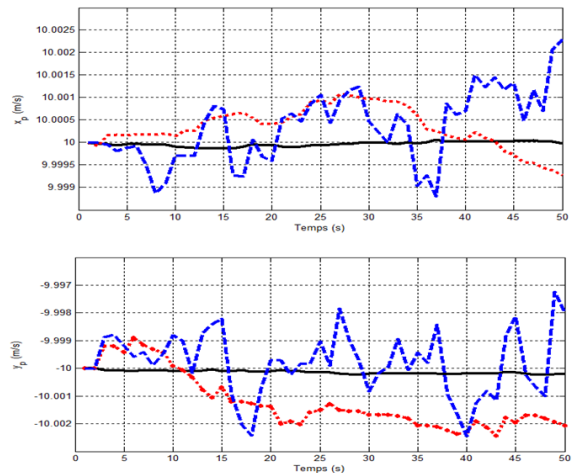


Fig. 3. Example 1: Evolution of the velocity (\dot{x} above and \dot{y} below). Black: Real velocity. Red: BPF. Blue: PBPf.

tion compared to a BPF. When the division of the non-measured is over, the wider box between x and y , which are the measured-variables, is bisected.

	x MSE (10^{-4})	\dot{x} MSE (10^{-7})	y MSE (10^{-3})	\dot{y} MSE (10^{-6})	Time (s)
BPF	1.44	2.50	5.01	1.69	20.32
PBPf	1.21	4.90	0.969	0.81	14.97

Table 1: Example 1: Comparison of the BPF and the PBPf for over 20 runs.

Figures 2 and 3 present the state trajectories estimated by the two algorithms for 10 boxes, where the solid black line

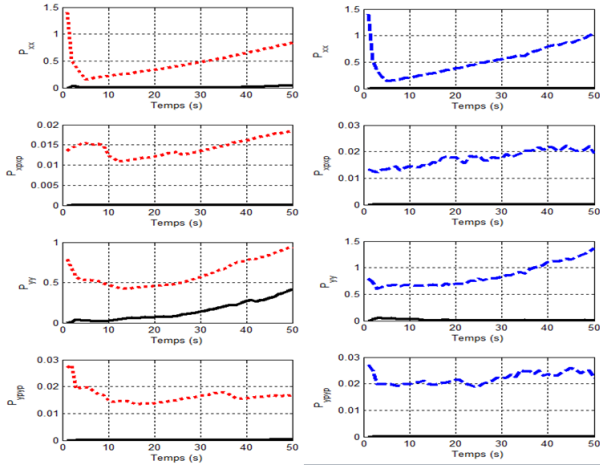


Fig. 4. Example 1: Evolution of the covariances. First row: P_{xx} . Second: $P_{\dot{x}\dot{x}}$. Third: P_{yy} . Last: $P_{y\dot{y}}$. Red: BPF. Blue: PBPF.

is the true value for simulations, the red dashed line are the results from the BPF and the blue dashed line is for the new filter. Both of them can track very well the true values. In Table 1, the average results of mean-square error (MSE) of states and CPU time of all iterations for over 20 runs are presented. The average MSEs of states for the two filters are very close to each other, while our algorithm presents some improvement over the BPF. However, in both filters, the covariances are increasing as illustrated in Figure 4. This is due to the fact that uncertainties depend on the range. The higher the distance is, the higher uncertainties are. In Figure 5, it is easy to notice that $\Delta x > \Delta x$ and that $\Delta y > \Delta y$. Therefore, covariances can't converge. That is why, on the next simulations, we will treat a new propagation equation.

4.2 Example 2

In this example, a new propagation equation is considered (taken from Bo et al. (2013) and adapted):

$$X_{k+1} = \begin{bmatrix} x_k + \Delta_t \dot{x}_k \\ \dot{x}_k + \Delta_t (-k_0 x_k (1 + k_d x_k^2) - c \dot{x}_k) \\ y_k + \Delta_t \dot{y}_k \\ \dot{y}_k + \Delta_t (-k_0 y_k (1 + k_d y_k^2) - c \dot{y}_k) \end{bmatrix} + \Gamma w_k \quad (17)$$

where Γ , X_k and w_k remain the same as in Example 1. The simulations are done with $\Delta t = 0.1s$; $k_0 = 1.5$; $k_d = 3$; $c = 1.24$; $|w_{k,x}| \leq 0.003$; $|w_{k,y}| \leq 0.003$; $|v_k^\theta| \leq 0.015$; $|v_k^d| \leq 0.025$; $|v_k^d| \leq 0.025$. The total simulation time is 100 s. The true initial and the initial state estimation are set to $x_0 = \hat{x}_0 = [0.2, 0.3, -0.2, 0.3]^T$. The variance-covariance matrix is initialized at $P_0 = \text{diag}\{0.01, 0.01, 0.01, 0.01\}$.

Moreover, in order to accentuate the effect presented in Figure 1 (the fact that the proposed filter is less pessimistic than the BPF for measured variables), a new measurement is added in comparison to Example 1. Now, the measurement vector is defined as $y_k = [\theta_k \ d_k \ \dot{d}_k]^T$, where θ_k and d_k are noisy measurements of the target bearing and range from the origin of the plane (as defined in (15) and (16)), and the radial speed \dot{d}_k is defined as:

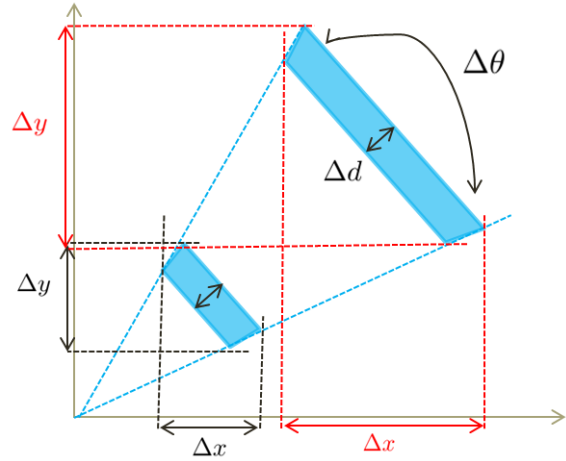


Fig. 5. Example 1: Illustration of the dependence uncertainties-range. Dashed blue: $\Delta\theta$ bounded by θ_{min} and θ_{max} . Solid blue: measurement (include θ and d).

$$\dot{d}_k = \sqrt{\dot{x}_k^2 + \dot{y}_k^2} + v_k^d \quad (18)$$

Then, R is defined as:

$$R = \begin{bmatrix} r^\theta & 0 & 0 \\ 0 & r^d & 0 \\ 0 & 0 & r^{\dot{d}} / \Delta t \end{bmatrix} \quad (19)$$

	x MSE (10^{-5})	\dot{x} MSE (10^{-6})	y MSE (10^{-6})	\dot{y} MSE (10^{-6})	Time (s)
BPF	1.024	7.840	2.890	3.610	256
PBPF	0.401	2.890	1.210	3.240	96

Table 2: Comparison of BPF and the PBPF filter for the new propagation fonction.

Figure 6 shows two of the state trajectories for 10 boxes. The two other results are quite similar. As it can be seen, the new filter is more precise and the CPU time is lower than the BPF. In Table 2, the average results of mean-square error (MSE) of states and CPU time of all iterations for over 20 runs are presented. The average MSEs of states for the two filters are very close to each other, while our algorithm still shows some improvements compared to the BPF. The covariances of both filters are converging in this example, see Figure 7 and the guaranteed bounds of y are presented in Figure 8.

5. CONCLUSIONS

In this paper, an improvement of the Box Particle Filter (BPF) base on polytopic measurement updating is proposed. Different examples of application have been compared with the BPF and the results are promising: the estimate is more precise and the computing time is lower than in the BPF.

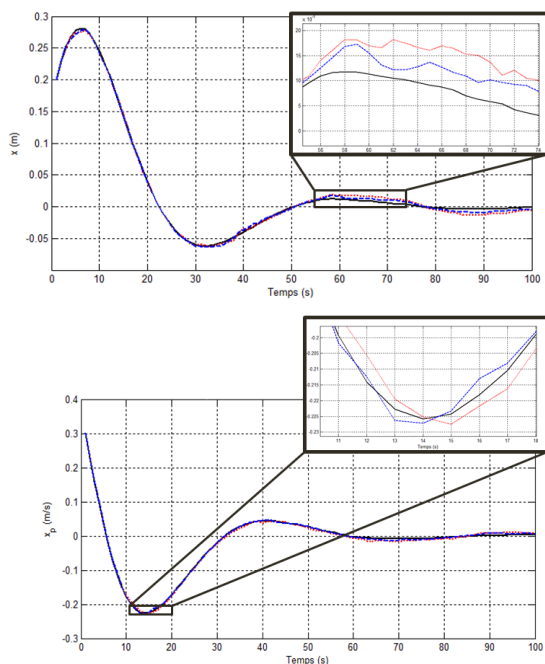


Fig. 6. Example 2: States trajectories. Above: x . Below: \dot{x} . Solid black : real value. Dashed red: BPF. Dashed blue: PBPF.

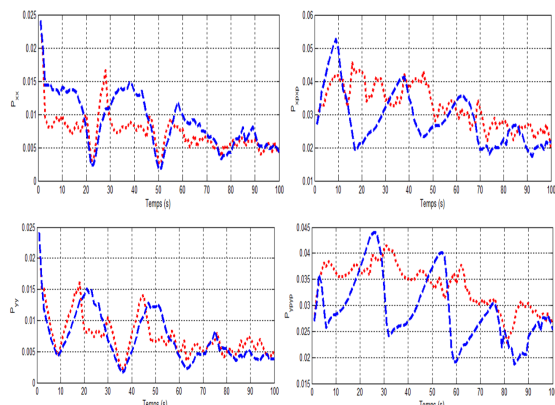


Fig. 7. Example 2: Evolution of the covariances. Up-left: P_{xx} . Up-right: $P_{\dot{x}\dot{x}}$. Down-left: P_{yy} . Down-right: $P_{\dot{y}\dot{y}}$. Dashed red: BPF. Dashed blue: PBPF.

Future work would include analysis of the computation of the bounds on measurements providing the best compromise between reliability and precision. Evaluation of weights depending on other characteristics than the volume of the resulting polytopes is also under study.

REFERENCES

Fahed Abdallah, Amadou Gning, and Philippe Bonnifait. Box particle filtering for nonlinear state estimation using interval analysis. *Automatica*, 44(3):807–815, 2008.

Zhou Bo, Qian Kun, MA Xu-Dong, and DAI Xian-Zhong. A new nonlinear set membership filter based on guaranteed bounding ellipsoid algorithm. *Acta Automatica Sinica*, 39(2):146–154, 2013.

Neil J Gordon, David J Salmond, and Adrian FM Smith. Novel approach to nonlinear/non-gaussian bayesian state estimation. In *IEE proceedings F (radar and signal processing)*, volume 140, pages 107–113. IET, 1993.

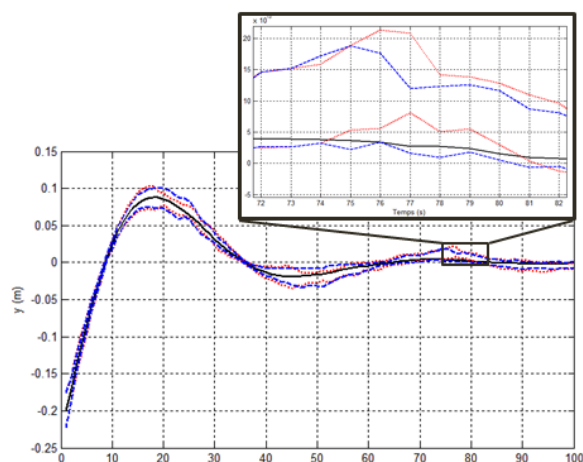


Fig. 8. Example 2: Guaranteed bounds of y . Solid black : real value. Dashed red: BPF. Dashed blue: PBPF.

Luc Jaulin. Applied interval analysis: with examples in parameter and state estimation, robust control and robotics, 2001.

Simon J Julier and Jeffrey K Uhlmann. New extension of the Kalman filter to nonlinear systems. In *AeroSense '97*, pages 182–193. International Society for Optics and Photonics, 1997.

Rudolph Emil Kalman et al. A new approach to linear filtering and prediction problems. *Journal of basic Engineering*, 82(1):35–45, 1960.

Jean B Lasserre. An analytical expression and an algorithm for the volume of a convex polyhedron in n . *Journal of optimization theory and applications*, 39(3): 363–377, 1983.

Boris T Polyak, Sergey A Nazin, CéCile Durieu, and Eric Walter. Ellipsoidal parameter or state estimation under model uncertainty. *Automatica*, 40(7):1171–1179, 2004.

Eelco Scholte and Mark E Campbell. A nonlinear set-membership filter for on-line applications. *International Journal of Robust and Nonlinear Control: IFAC-Affiliated Journal*, 13(15):1337–1358, 2003.

Rudolph Van Der Merwe, Arnaud Doucet, Nando De Freitas, and Eric A Wan. The unscented particle filter. In *Advances in neural information processing systems*, pages 584–590, 2001.

Balder Von Hohenbalken. Least distance methods for the scheme of polytopes. *Mathematical Programming*, 15(1): 1–11, 1978.

E Walter and Hélene Piet-Lahanier. Exact recursive polyhedral description of the feasible parameter set for bounded-error models. *IEEE Transactions on Automatic Control*, 34(8):911–915, 1989.

Peng Wang, Philippe Xu, Philippe Bonnifait, and Jianwen Jiang. Box particle filtering for slam with bounded errors. In *2018 15th International Conference on Control, Automation, Robotics and Vision (ICARCV)*, pages 1032–1038. IEEE, 2018.

Joe Warren. Barycentric coordinates for convex polytopes. *Advances in Computational Mathematics*, 6(1):97–108, 1996.